Available online at www.sciencedirect.com
ScienceDirect
Journal of Power Sources 181 (2008) 24–30
JOURNAL OF POWER SOURCES
www.elsevier.com/locate/jpowsour

Electrochemical behavior of CO, CO_2 and methanol adsorption products formed on Pt–Rh alloys of various surface compositions

Hanna Siwek [a], Wojciech Tokarz [a], Piotr Piela [a], Andrzej Czerwiński [b,*]

[a] *Industrial Chemistry Research Institute, Rydygiera 8, 01-793 Warsaw, Poland*
[b] *Faculty of Chemistry, Warsaw University, Pasteura 1, 02-093 Warsaw, Poland*

Received 5 September 2007; received in revised form 24 October 2007; accepted 13 November 2007
Available online 21 November 2007

Abstract

CO, CO_2 and methanol adsorption/electro-desorption processes have been studied on Pt–Rh alloy electrodes with various surface compositions and on the pure Pt and Rh electrodes. Pt–Rh alloys are slightly more tolerant to poisons from these molecules' adsorption compared to pure Pt and Rh.

The values of electrode coverage by the adsorption products and the values of the average electron-per-site (*eps*) parameter obtained from stripping voltammetry suggest some differences exist between the adsorption layers formed depending on the adsorbing molecule, the electrode's surface composition and the adsorption conditions. The observations could be rationalized by considering the differences in adsorption mechanisms of CO, CO_2 and methanol and by taking the adsorption products to be uniquely bridge-bonded and on-top-bonded CO.

There is no direct correlation between the average *eps* parameter and the stability of the adsorption layer. Adsorption layers formed on an electrode with a given surface composition and characterized by the same value of the average *eps* parameter can have different potential stability, if they were formed by different molecules or under different conditions.

Keywords: Carbon oxides; Methanol; Adsorption; Alloys; Platinum; Rhodium

1. Introduction

Studies of small organic molecule (SOM) adsorption and electro-desorption from solid platinum-based electrodes are related to technology advancement in important practical applications of electrochemistry. These include anode electro-catalysis for direct oxidation fuel cells, e.g., direct methanol fuel cells (DMFCs) [1–3] and reformate fuel cells [4], and electro-chemical CO_2 scrubbing. [5]

For example, methanol electro-catalysis in DMFCs currently relies on binary platinum–ruthenium alloy catalysts. Ruthenium is introduced to platinum as a metal that, firstly, has a greater ability, compared to Pt, to form surface oxygen species needed to fully oxidize methanol (bi-functional effect [6]), and secondly, has a lower d-band electron density than Pt and, thus, is capable of weakening the bond between a strongly adsorbed oxidation intermediate and Pt by withdrawing electron density from the bond (the ligand effect [7]). Despite the much better performance of Pt–Ru compared with Pt and many other binary Pt-based catalysts, the methanol anode activation continues to be the largest voltage loss in the DMFC. It is therefore necessary to carefully look into the mechanism of methanol electro-oxidation on such binary alloys in order to devise better electro-catalysts.

Pt–Rh is a model binary Pt-based catalyst suitable for SOM electrode reactions studies. It is a homogeneous alloy and its surface composition can be easily measured and tuned in the whole range. [8] In this contribution we present the results of a comparative study of CO, CO_2 and methanol adsorption/electro-desorption at Pt–Rh electrodes focusing mostly on the influence of alloy composition on the nature of adsorption products.

2. Experimental

All electrodes used in this study were limited volume electrodes (LVEs) [9–11], which were electrodeposited poten-

* Corresponding author. Tel.: +48 22 568 24 43/822 02 11x305; fax: +48 22 568 23 90.
E-mail addresses: andrzej.czerwinski@ichp.pl, aczerw@chem.uw.edu.pl (A. Czerwiński).

0378-7753/$ – see front matter © 2007 Elsevier B.V. All rights reserved.
doi:10.1016/j.jpowsour.2007.11.033

tiostatically on 0.5-mm diameter gold wires (99.99 Au) from aqueous solutions containing H_2PtCl_6, $RhCl_3$ and HCl. The electro-deposition potential was 0.180 V *vs.* SHE in all cases. The deposited layer thickness was a few micrometers and the surface roughness factor was in the range 50–200. The procedure for obtaining a Pt–Rh electrode surface with a precisely defined surface composition is described in detail in ref. [8].

All electrochemical studies were performed in deoxygenated aqueous 0.5 M H_2SO_4 solutions at room temperature. The stripping technique was used for studying the adsorption of methanol and carbon oxides. [12] For CO and CO_2 adsorption, a pressure of 1 bar of the respective gas was maintained during the adsorption step, after which the gas was thoroughly flushed from the cell with nitrogen or argon. In the case of methanol adsorption, a concentration of 1 M methanol was used. After the adsorption step, the methanol was removed from the cell by replacing the methanol-containing electrolyte with a fresh, deoxygenated portion of the supporting electrolyte taking special care that no oxygen be introduced into the cell.

All chemicals and gases used were of high-purity grade and were used without additional purification. Prior to adsorption the electrodes were cleaned by *in situ* electrochemical cycling to obtain well-defined voltammograms certifying high system purity.

Electrochemical techniques were performed with a VoltaLab PGZ 301 potentiostat/galvanostat. Unless noted otherwise, in cyclic voltammetry experiments, a scan rate of 50 mV s^{-1}, an anodic vertex potential of +1.250 V *vs.* SHE and a cathodic vertex potential of +0.050 V *vs.* SHE were used. The working electrode potential was measured against a mercury/mercury sulfate or a silver/silver chloride reference electrode, but all the potentials are given *vs.* SHE.

3. Results and discussion

3.1. General considerations

In order to point out major similarities and differences between the adsorption processes of CO, CO_2 and methanol, general schemes of the processes are provided in Fig. 1. In the case of CO adsorption on a metal surface with suitable affinity to carbonaceous adsorbates, such as the alloys studied here, the process is likely a simple chemical adsorption without charge transfer over distances longer than the length of the metal–carbon bond (Fig. 1a). It is known from spectroscopic studies that the CO adsorption product is either a CO molecule bonded linearly *via* the carbon atom on top of a single adsorption site (metal atom), or the same molecule bonded to two adjacent adsorption sites with the carbon atom forming a bridge between them. [13]

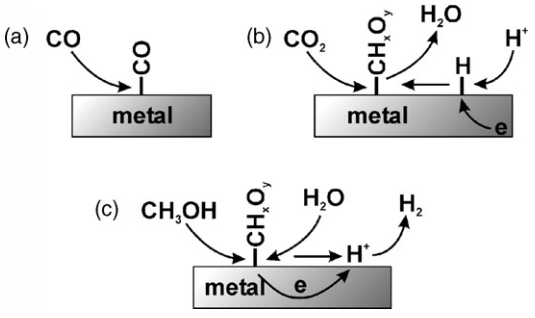

Fig. 1. General adsorption reaction scheme for (a) CO, (b) CO_2 and (c) methanol adsorption on the electrode surface.

CO_2 adsorption is a much more complicated process, because it can only proceed with electron transfer from the electrode to the CO_2 molecule *via* adsorbed hydrogen (Fig. 1b): [14]

$$(x-2y+4)H^+ + (x-2y+4)e \rightarrow (x-2y+4)H_{(ads)} \quad (1)$$

$$CO_2 + (x-2y+4)H_{(ads)} \rightarrow CH_xO_{y(ads)} + (2-y)H_2O \quad (2)$$

It is therefore a reductive adsorption requiring more than one adsorption site to complete a single molecule adsorption act. In the case of CO_2 adsorption on platinum metals it is usually assumed that $x=0$ and $y=1$, meaning $CO_{(ads)}$ is the only adsorption product, just as in the case of CO adsorption. [15] However, given the complexity of the process and considering some previous radiometric results [16], one simple product is unlikely.

Although, unlike CO_2 adsorption, methanol adsorption does not require a source of or sink for electrons such as the external circuit, it is also a charge-transfer, this time oxidative adsorption process, in which molecular hydrogen is evolved (Fig. 1c):

$$CH_3OH + (y-1)H_2O \rightarrow CH_xO_{y(ads)} + (2y-x+2)H^+ + (2y-x+2)e \quad (3)$$

$$(2y-x+2)H^+ + (2y-x+2)e \rightarrow (y-x/2+1)H_2 \quad (4)$$

In the case of methanol adsorption on Pt it has been found by spectroscopy that the deviation from $x=0$ and $y=1$, if any, is very small. [17–19] However, such data for other metal surfaces, particularly alloy surfaces, is missing. By comparing the CO_2 and the methanol adsorption processes (Fig. 1b and c), one can suspect a certain similarity in the products formed, because in both cases adsorbate formation requires an ensemble of adsorption sites with the sites adjacent to the $CH_xO_{y(ads)}$-binding site being involved in atomic hydrogen adsorption.

In the present work, the *eps* (electrons per site) parameter is used to characterize the CO, CO_2 and methanol adsorption products. It is the number of electrons required to oxidatively remove the adsorbate molecules from the adsorption sites, taken for one adsorption site. If one assumes, which can be safely done in the case of the studied molecules, that the oxidative removal of the carbonaceous adsorbate leads to exclusive formation of gaseous CO_2, then, for $CH_xO_{y(ads)}$, the *eps* is given by the following equation:

$$\text{eps} = \frac{x+2(2-y)}{n} \quad (5)$$

where n is the number of sites blocked by one molecule of the adsorbate. "Blocking" in that sense is either forming a chemical bond with the site or making the site unavailable for adsorption due to space limitation and/or electronic interaction. Conse-

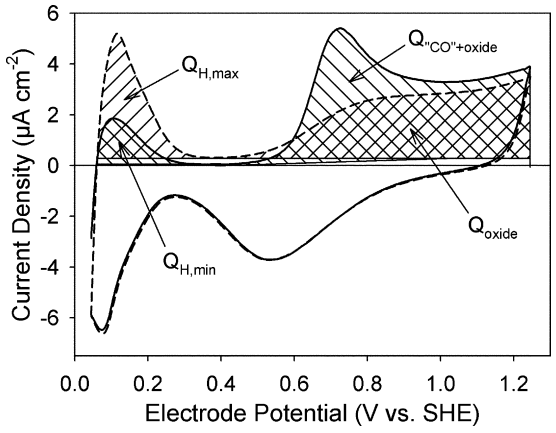

Fig. 2. Charges analysis of a stripping cyclic voltammetry experiment. Thick, solid line is the stripping cycle. Thick, dashed line is the cycle immediately following the stripping cycle.

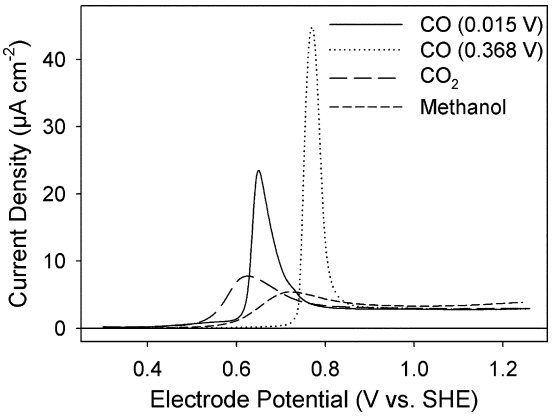

Fig. 3. Stripping scans of the CO, CO_2 and methanol adsorption products from Pt–Rh (60% Rh). Two adsorption potentials are shown for CO. Curves descriptions and adsorption potential values for CO shown in graph. Adsorption potential for CO_2 and methanol was 0.01 and 0.20 V *vs.* SHE, respectively.

quently, when $CO_{(ads)}$ is the form of the adsorbate, for which $n = 1$ or 2 is expected, an *eps* value between 1 and 2 should be obtained. (In this case, *eps*-1 should give the fraction of sites binding $CO_{(ads)}$, for which CO is attached in the on-top position.) Experimental (average) *eps* values outside this range prove the adsorbate is, at least partially, something other than $CO_{(ads)}$.

Careful treatment of the stripping voltammetry data obtained in this work allows for precise calculation of the average *eps* parameter. Fig. 2 presents the details of the analysis using an example methanol stripping experiment performed with a Pt–Rh alloy electrode. Some assumptions presented in detail in ref. [8] lead to the formula for the experimental *eps*:

$$\text{eps} = \frac{(Q_{\text{“CO”}+\text{oxide}} - Q_{\text{oxide}})[0.59x_{\text{Rh}} + 0.77(1 - x_{\text{Rh}})]}{(Q_{\text{H,max}} - Q_{\text{H,min}})} \quad (6)$$

where x_{Rh} is the electrode's surface molar fraction of Rh. The same assumptions lead to calculation of the electrode's coverage by the carbonaceous adsorbate, θ, using the following formula:

$$\theta = 1 - \frac{Q_{\text{H,min}}}{Q_{\text{H,max}}} \quad (7)$$

Fig. 3 is used to illustrate the fact that there are important differences in the nature of the adsorption products formed on a Pt–Rh alloy surface, 60%-Rh in this case, during CO, CO_2 and methanol adsorption. The position of the stripping peak on the potential scale and the sharpness of the peak are respectively a measure of the stability and uniformity of the adsorption layer. CO adsorption gives rise to sharp electro-desorption peaks, the position of which depends strongly on the adsorption potential (solid and dotted lines in Fig. 3). CO_2 and methanol adsorption products both generate wide peaks, yet positioned differently on the potential scale (long-dashed and short-dashed lines). In view of the spectroscopic evidence in favor of similarity of the adsorption products for all three SOMs it is interesting to investigate further the differences in electrochemical behavior.

3.2. *Influence of adsorption potential*

Fig. 4 presents the influence of adsorption potential on the coverage of a *ca.* 30%-Rh Pt–Rh electrode by adsorption products for all three investigated molecules. There is a different pattern for each adsorbing substance reflecting mostly the different mechanisms of adsorption (Fig. 1). Coverage for CO is high and constant with adsorption potential reflecting the fact that CO, being a stronger ligand than H for both Pt and Rh, is able to efficiently displace adsorbed hydrogen ($H_{(ads)}$) from the surface of the alloy. CO_2 adsorption products require $H_{(ads)}$ to form, therefore as the adsorption potential is lowered and enters the $H_{(ads)}$ region for the electrode, the coverage rises. It is interesting that for all adsorption potential values below 0.200 V *vs.* SHE, the coverage for CO_2 reaches the saturation coverage despite the fact that coverage of the electrode by $H_{(ads)}$ in the absence of a carbonaceous adsorbate changes gradually with electrode potential. A similar behavior has been observed before for pure platinum, for which it was shown that as soon as there is weakly adsorbed hydrogen available on the surface, *i.e.* below *ca.* 0.200 V *vs.* SHE, the saturation electrode cover-

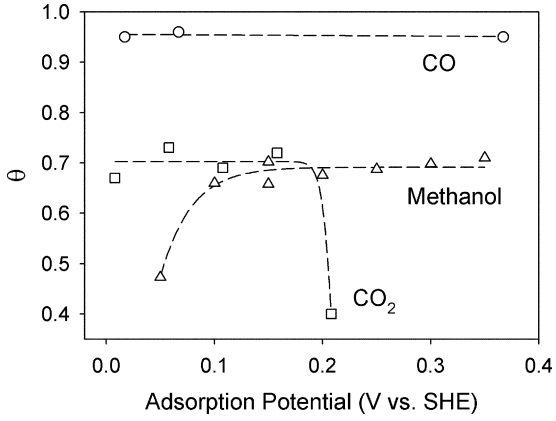

Fig. 4. Pt–Rh (*ca.* 30% Rh) electrode coverage by adsorption products *vs.* adsorption potential for CO (circles), CO_2 (squares) and methanol (triangles) adsorption.

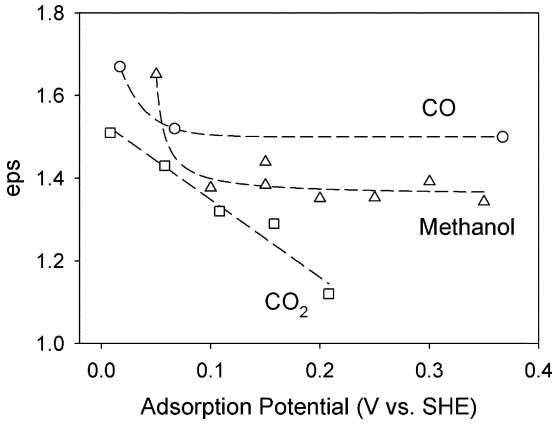

Fig. 5. Electron-per-site (*eps*) parameter *vs.* adsorption potential for CO (circles), CO_2 (squares) and methanol (triangles) adsorption products formed on Pt–Rh (*ca.* 30% Rh).

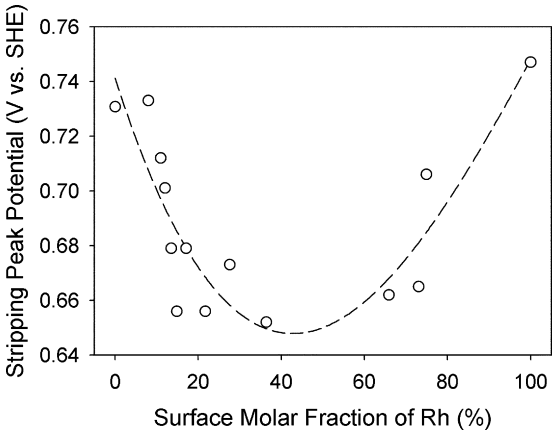

Fig. 6. Stripping peak potential *vs.* Pt–Rh alloy surface composition for CO adsorption products. Adsorption potential 0.07 V *vs.* SHE.

age by the CO_2 adsorption products is attained [20,21]. During CO_2 adsorption at a relatively high electrode potential, there is formation of new weakly adsorbed $H_{(ads)}$ for reaction with CO_2 until a saturation state (coverage by CO_2 adsorption products) is attained [22]. Finally, the coverage of the electrode by methanol adsorption products stays at its maximum in a wide range of adsorption potential and becomes lower only at very low adsorption potential. Methanol, just as CO, competes with $H_{(ads)}$ for bare metal sites during adsorption, however, being a molecule with an outer "layer" built of hydrogen atoms and, hence, possessing a ligand strength similar to H, it is unable to displace $H_{(ads)}$ as efficiently as CO is. Because the availability of free sites becomes small as the electrode potential is lowered to 0.050 V *vs.* SHE due to increasing coverage by $H_{(ads)}$, the saturation coverage by methanol adsorption products at this low adsorption potential will likely be lower than at a higher adsorption potential. Existing ability of methanol to displace $H_{(ads)}$ is apparent from the high and adsorption-potential-independent values of coverage in the adsorption potential range between 0.100 and 0.350 V *vs.* SHE. A possible displacement mechanism, operative for both methanol and CO, might involve weakening of the metal–$H_{(ads)}$ bond at the $H_{(ads)}$ sites neighboring the $CH_xO_{y(ads)}$ site, due to an electronic effect. Such affected $H_{(ads)}$ sites would be more susceptible to spontaneous $H_{(ads)}$ desorption and subsequent attack of a solution molecule of methanol on the bare site.

Fig. 5 includes the values of the average *eps* parameter obtained using different adsorption potentials at the *ca.* 30%-Rh Pt–Rh alloy electrodes. Firstly, the *eps* values differ for CO, CO_2 and methanol adsorption products attesting to existing differences in the chemical nature of the products. Secondly, it is seen that for all three substances the eps values tend to increase as the adsorption potential is lowered. Two interpretations can be offered for the latter observation. The increasingly reducing conditions at the electrode surface when the potential is lowered (abundance of $H_{(ads)}$) could favor formation of a more reduced adsorption product, thus increasing the average *eps*. The second hypothesis involves bridge-bonded and on-top-bonded CO as the only adsorption products in each case. Increased presence of $H_{(ads)}$ at the low adsorption potential would make the formation of bridge-bonded CO less favorable and, as a result, the average *eps* would rise. The data presented here cannot scrutinize between these two interpretations.

3.3. Influence of Pt–Rh alloy's surface composition

The surface composition of Pt–Rh electrodes has a marked influence on CO stripping. Fig. 6 shows the stripping peak potential *vs.* surface molar fraction of Rh in the alloy for CO adsorption at 0.07 V *vs.* SHE, *i.e.*, in the presence of initial high electrode coverage by $H_{(ads)}$. It is seen that in this case Pt–Rh alloys exhibit a lowering of the peak potential relative to pure Pt and Rh metals. The maximum lowering amounts to *ca.* 100 mV and it is for alloys possessing between 20 and 60% Rh. The corresponding values of electrode coverage by adsorbed CO and of the average *eps* are presented in Fig. 7. The coverage slightly falls as the fraction of Rh is increased; nevertheless its value remains high even for pure Rh ($\theta = 90\%$). The *eps* parameter shows a maximum in the region of alloy surface compositions, for which there is maximum lowering of the stripping peak potential (Fig. 6).

This behavior can be rationalized by assuming that the CO adsorption product is either bridge-bonded or on-top-bonded CO. The former yields an *eps* equal to 1 and should be more

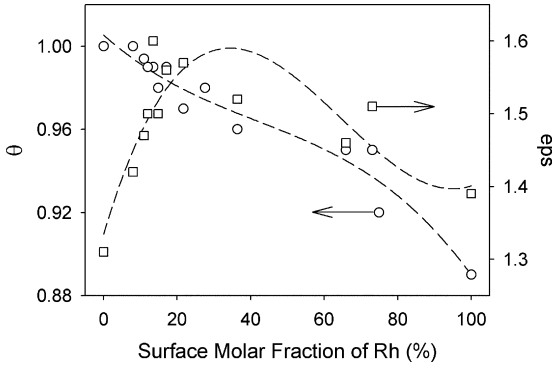

Fig. 7. Electrode coverage by adsorption products (circles) and electron-per-site (*eps*) parameter (squares) for CO adsorption products *vs.* Pt–Rh alloy surface composition. Adsorption potential 0.07 V *vs.* SHE.

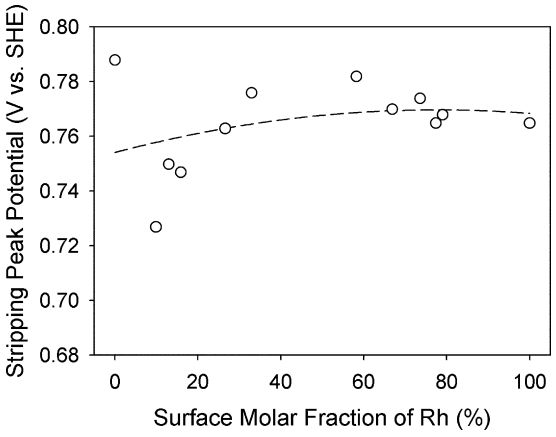

Fig. 8. Stripping peak potential *vs.* Pt–Rh alloy surface composition for CO adsorption products. Adsorption potential 0.37 V *vs.* SHE.

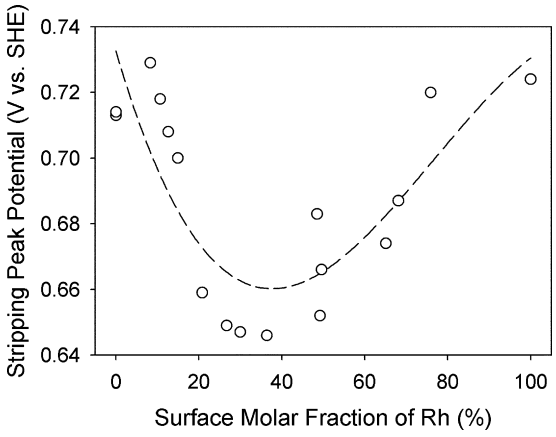

Fig. 10. Stripping peak potential *vs.* Pt–Rh alloy surface composition for CO_2 adsorption products. Adsorption potential 0.07 V *vs.* SHE.

stable on the electrode's surface, whereas the latter, resulting in *eps* equal to 2, should be more prone to electro-desorption. Formation of bridge-bonded CO with the bridge joining a Pt and a Rh atom is less favorable energetically than the case when the bridge is between two atoms of the same element, *i.e.*, two Pt or two Rh atoms. (The first situation has a broken symmetry.) The relationships presented in Figs. 6 and 7 can be considered a consequence of the fact that the intermediate-composition Pt–Rh alloys have the largest number of adsorption sites where a Pt atom neighbors a Rh atom (it is a homogeneous alloy).

In order to confirm that such behavior is typical for CO adsorption, a different adsorption potential has been used, this time from the double layer region of the CVs (0.37 V *vs.* SHE). The dependence of the stripping peak potential on the surface composition of the alloy for this case is shown in Fig. 8. Fig. 9 includes the corresponding θ and *eps* values. It is seen from Fig. 8 that this time the lowering of the peak potential for intermediate-composition surfaces is absent. On both the pure metals and on the alloys in the full range of surface composition the peak is observed at around 0.76 V *vs.* SHE. At the same time the relationships from Fig. 9 are almost identical to those from Fig. 7. This somewhat different behavior than observed in the case of CO adsorption in the presence of $H_{(ads)}$ shows that, although the average *eps* might be a function of surface composition only, the stability of the adsorption layer formed is influenced additionally by the adsorption conditions. One could assume, as a hypothesis, that depending on the activity of $H_{(ads)}$ during CO adsorption the structure of the resulting adsorption layer would be different. Perhaps, adsorption in the absence of $H_{(ads)}$ leads to a more uniform layer, which is more resistant to oxidation. This view finds support in the shape of stripping CVs obtained for CO adsorbed at two potentials shown in Fig. 3. The stripping peak for CO adsorption products formed in the absence of $H_{(ads)}$ is narrow and tall compared to the peak recorded after CO adsorption on the surface of the same electrode (60% Rh) but in the presence of $H_{(ads)}$. A sharp electro-desorption peak attests to an energetically uniform adsorbate. Such effects of different adsorption layer structure in the case of CO adsorption on Pt(1 1 1) have been recently quantified using the modern sum frequency generation (SFG) spectroscopy. [23]

In the case of CO_2 adsorption on Pt–Rh surfaces, a lowering of the stripping peak potential relative to the potentials recorded for the pure metals is also observed (Fig. 10). The maximum lowering is a little less than the maximum lowering found in the case of CO adsorption (*cf.* Fig. 6). Fig. 11 shows the values of electrode coverage by CO_2 adsorption products and of the average *eps* parameter, both as a function of electrode's surface composition. Contrary to CO adsorption, the electrode coverage is now

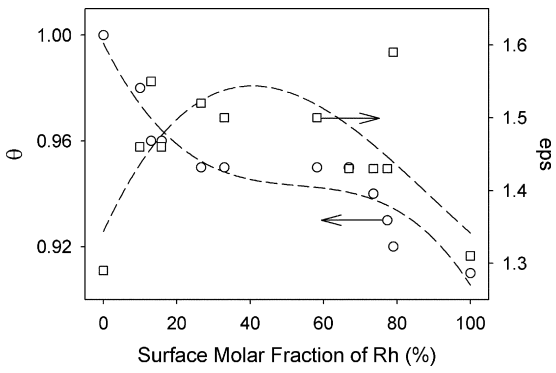

Fig. 9. Electrode coverage by adsorption products (circles) and electron-per-site (*eps*) parameter (squares) for CO adsorption products *vs.* Pt–Rh alloy surface composition. Adsorption potential 0.37 V *vs.* SHE.

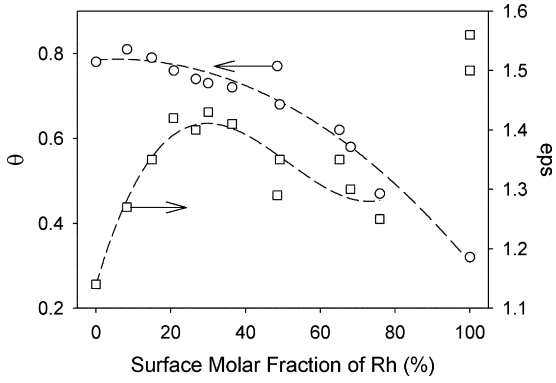

Fig. 11. Electrode coverage by adsorption products (circles) and electron-per-site (*eps*) parameter (squares) for CO_2 adsorption products *vs.* Pt–Rh alloy surface composition. Adsorption potential 0.07 V *vs.* SHE.

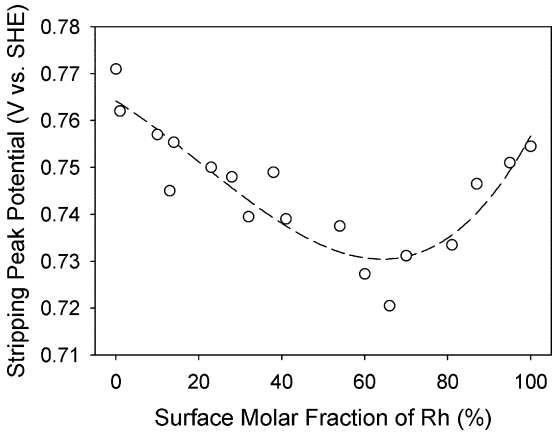

Fig. 12. Stripping peak potential *vs.* Pt–Rh alloy surface composition for methanol adsorption products. Adsorption potential 0.20 V *vs.* SHE.

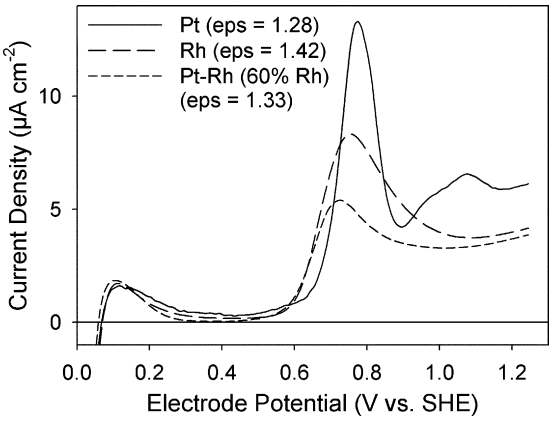

Fig. 13. Stripping scans of the methanol adsorption products from Pt, Rh and Pt–Rh (60% Rh). Curves descriptions and corresponding electron-per-site (*eps*) values shown in graph.

strongly dependent on the surface fraction of Rh. The maximum coverage is observed for pure Pt and it is significantly lower than in the case of CO adsorption (*cf.* Figs. 7 and 9). The coverage falls with the Rh content reaching only 0.3 for pure Rh. Those differences between CO and CO_2 adsorption clearly originate from the different adsorption mechanisms of these molecules (*cf.* Fig. 1). CO_2 adsorption is a reactive adsorption process involving an ensemble of adjacent sites (likely at least two with $H_{(ads)}$). Because of limited possibilities for surface rearrangement of the adsorbate, the availability of such ensembles of sites falls very fast as the adsorption process proceeds. Thus, lowered saturation coverage is attained. It is possible that the surface rearrangement becomes even more difficult when the content of Rh increases, which would explain the lowering of θ with Rh content.

As to the *eps*, its values are generally a little lower than in the case of CO adsorption products. Assuming the bridge-bonded and the on-top-bonded CO as the only adsorption products also in the case of CO_2 adsorption, the lower average *eps* values could be explained by the fact that a higher probability for a CO_2 adsorption act exists in areas where there are multiple reactive $H_{(ads)}$. These are likely areas of multiple adjacent Pt atoms, where, at the same time, there should be a tendency to form bridge-bonded CO (see earlier discussion of Fig. 7). The small difference in the maximum lowering of the stripping peak potential between CO and CO_2 (*cf.* Figs. 6 and 10) is in line with the small differences in the *eps* values and the bridge-bonded/on-top-bonded CO concept (compare discussion of Figs. 6 and 7). The shape of the relationship between the *eps* and surface composition is similar for CO and CO_2 and it could be explained as before. One marked difference is in the region of high Rh content, pure Rh in particular. For CO_2 adsorption products the *eps* for 100% Rh is the highest. A possible explanation for this can be arrived at by noticing the low coverage by the adsorption products for CO_2 on Rh (0.3), which corresponds to a simultaneous high coverage by $H_{(ads)}$, and by recalling the influence of $H_{(ads)}$ on the *eps* parameter (*cf.* Fig. 5 and discussion thereof).

Fig. 12 includes the relationship between the stripping peak potential and the surface fraction of Rh for the methanol adsorption products. A slight lowering of the peak potential in the case of the Pt–Rh alloys relative to the pure metals is also present in the case of methanol, however, the maximum lowering is merely 40 mV. Fig. 13 presents stripping voltammograms recorded for Pt, Rh and a Pt–Rh (60% Rh) alloy surface. The corresponding average *eps* values of 1.28, 1.42 and 1.33 do not differ much and are similar to the *eps* values obtained for CO_2 adsorption (lower than the values for CO adsorption). In spite of these similarities the adsorption layer formed during methanol adsorption is more difficult to oxidize compared to the CO_2 adsorption layer. This proves again that the same average *eps* value might correspond to more than one adsorption layer structure. Each such structure can be characterized by a different energetic stability and might produce a different stripping CV. The difference found for CO_2 and methanol can reflect the differences in adsorption mechanisms of these molecules (*cf.* Fig. 1). CO_2 searches for $H_{(ads)}$ sites to adsorb on, while methanol requires bare metal sites. Because for Pt–Rh alloy surfaces such local areas likely differ in composition and catalytic reactivity, the final results of the adsorption processes—the adsorption layers (and their electro-desorption image) may differ as well.

4. Conclusions

Precise adjustment of electrode's surface composition possible for Pt–Rh alloys allowed for detailed studies of CO, CO_2 and methanol adsorption/electro-desorption on this Pt–M alloy. Pt–Rh alloys were found to be slightly more tolerant to poisons from these molecules' adsorption compared to pure Pt and Rh, as judged from the position of the stripping peak on the potential scale.

The values of electrode coverage by the adsorption products (θ) and the values of the average electron-per-site parameter (*eps*) calculated from the stripping CVs point to some differences existing between the adsorption layers formed depending on the adsorbing molecule, the electrode's surface composition and the adsorption conditions. CO adsorption products have higher *eps* and θ than CO_2 and methanol adsorption products. Intermediate-composition alloy surfaces tend to produce higher-*eps* products than one-component-enriched alloy surfaces. The presence of $H_{(ads)}$ during adsorption always results in a higher *eps*. These

observations as well as the values of the *eps* parameter always falling in the range from 1.0 to 2.0 could be understood by considering the differences in adsorption mechanisms of CO, CO_2 and methanol and by taking the adsorption products to be uniquely bridge-bonded and on-top-bonded CO. Although the latter assumption was sufficient, the presence of adsorbates more reduced or more oxidized than $CO_{(ads)}$ cannot be excluded based on the data.

It was further shown that there is no direct correlation between the average *eps* parameter and the energetic stability of the adsorption layer (stripping peak potential). Although very often the high-*eps* adsorption product is easier do oxidize than the low-*eps* product, another factor sometimes comes into play. This factor is related to the mechanism of adsorption of a particular molecule and to the conditions of the adsorption process. In consistence with some recent spectroscopic data [23], it was proposed that adsorption layers characterized by the same value of the average *eps* parameter but differing in structure might form under different conditions. The more uniform (ordered) the structure, the more difficult it is to electro-oxidize the layer.

Acknowledgements

Statutory funding from the Industrial Chemistry Research Institute, Warsaw and the Department of Chemistry, Warsaw University, is greatly acknowledged.

References

[1] A.S. Aricò, S. Srinivasan, V. Antonucci, Fuel Cells 1 (2001) 133.
[2] P. Piela, P. Zelenay, Fuel Cell Rev. 1 (2004) 17.
[3] S. Gottesfeld, Fuel Cell Rev. 1 (2004) 25.
[4] T.R. Ralph, M.P. Hogarth, Platinum Met. Rev. 46 (2002) 117.
[5] K.W. Frese Jr., in: B.P. Sullivan, K. Krist, H.E. Guard (Eds.), Electrochemical and Electrocatalytic Reactions of Carbon Dioxide, Elsevier, Amsterdam, 1993, p. 145.
[6] M. Watanabe, S. Motoo, J. Electroanal. Chem. 60 (1975) 275.
[7] Y. Tong, H.S. Kim, P.K. Babu, P. Waszczuk, A. Więckowski, E. Oldfield, J. Am. Chem. Soc. 124 (2002) 468.
[8] W. Tokarz, H. Siwek, P. Piela, A. Czerwiński, Electrochim. Acta 52 (2007) 5565.
[9] A. Czerwiński, S. Zamponi, R. Marassi, J. Electroanal. Chem. 304 (1991) 233.
[10] A. Czerwiński, R. Marassi, S. Zamponi, J. Electroanal. Chem. 316 (1991) 211.
[11] A. Czerwiński, R. Marassi, J. Sobkowski, Ann. Chim. Rome 74 (1984) 681.
[12] H.A. Gasteiger, N. Marković, P.N. Ross, E.J. Cairns Jr., J. Phys. Chem. 98 (1994) 617.
[13] B. Beden, A. Bewick, K. Kunimatsu, C. Lamy, J. Electroanal. Chem. 142 (1982) 345.
[14] A. Czerwiński, J. Sobkowski, J. Electroanal. Chem. 59 (1975) 41.
[15] B. Beden, A. Bewick, M. Razaq, J. Weber, J. Electroanal. Chem. 139 (1982) 203.
[16] J. Sobkowski, A. Czerwiński, J. Phys. Chem. 59 (1985) 365.
[17] S. Juanto, B. Beden, F. Hahn, J.M. Léger, C. Lamy, J. Electroanal. Chem. 237 (1987) 119.
[18] B. Beden, S. Juanto, J.M. Léger, C. Lamy, J. Electroanal. Chem. 238 (1987) 323.
[19] E. Morallón, A. Rodes, J.L. Vázquez, J.M. Pérez, J. Electroanal. Chem. 391 (1995) 149.
[20] A. Czerwiński, J. Sobkowski, A. Więckowski, Int. J. Appl. Radiat. Isot. 25 (1974) 295.
[21] J. Sobkowski, A. Więckowski, P. Zelenay, A. Czerwiński, J. Electroanal. Chem. 100 (1979) 781.
[22] J. Sobkowski, A. Czerwiński, J. Electroanal. Chem. Int. Electrochem. 55 (1974) 391.
[23] A. Lagutchev, G.Q. Lu, T. Takeshita, D.D. Dlott, A. Więckowski, J. Chem. Phys. 125 (2006) 154705.